Acta Materialia Turcica

Volume 4, July 2020, Pages 25-34

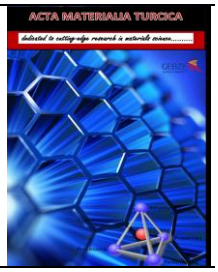

Complex Fluid Flow in Power Nuclear Reactors Cores; Cases of BWR, PBMR and HTR-PM

K. SIDI-ALI

Nuclear Research Centre of Draria, BP 43 Sebala, Draria, Algiers, Algeria

Abstract:

In this work, the technology of PBMR, HTR-PM and BWR as well as the nuclear reactor core constitution with fuel elements arrangement are presented. The mathematical part: conservation equations for continuity, momentum and energy as well as equations of state and boundary conditions, for both porous media theory and two-phase flow theory are developed and applied to each type of nuclear reactor. For the case of the HTR-PM and PBMR nuclear reactors, two approaches cases are applied. The first approach is the study of a channel saturated with a porous medium consisting of fuel spheres and cooled by an inert gas, to approach the HTR-PM. The second is an application for a case of porous medium consisting of the same fuel spheres but arranged in an annular domain to approach the PBMR. For the case of BWRs, a nuclear thermalhydraulic channel is defined and the different two-phase flows presented. The same set-up equation is applied except that it is written for each phase and for the interface between the two phases, the specific case of annular two-phase flow is studied. The obtained results, presented in figures and physically analyzed, are very satisfactory. It can thus be concluded that applying the model of porous media and the two-phase flow one for complex flows respectively for PBMR, HTR-PM or BWR power nuclear reactors core can ensure a good behavior of the nuclear reactor core thermalhydraulics.

Keywords: Nuclear reactors, Complex flows, HTR-PM, PBMR, BWR.

DOI:

1. INTRODUCTION

The cooling of nuclear reactor cores is the keystone of nuclear safety. Since the advent of the nuclear technology of GEN I, GEN II to GEN III and III+, nuclear reactors have evolved continuously. Each line and each generation has its own technology, design and nuclear safety requirements. An element common to all these generations and all these lines is ensuring the nuclear reactor core cooling whether in normal operation or in accidental one. Nuclear reactors using plate or cylindrical fuels and not operating under fluid phase change mode are easier to cool than other types of nuclear reactors. One takes the example of Pebble Bed Modular Reactors (PBMR), High Temperature Reactor-Pebble Modular (HTR-PM) or Boiling Water Reactor (BWR). For the first two nuclear reactors, the flow is so complex that the porous media theory approach has to be applied for all physical and thermalhydraulic calculations, whereas for the last nuclear reactor the two-phase flow theory approach is the only one that can provide a sure answer to physical and thermalhydraulic calculations of this type of nuclear reactor.

Corresponding Author E-mail: kamelsidiali@gmail.com

Acta Materialia Turcica

Volume 4, July 2020, Pages 25-34

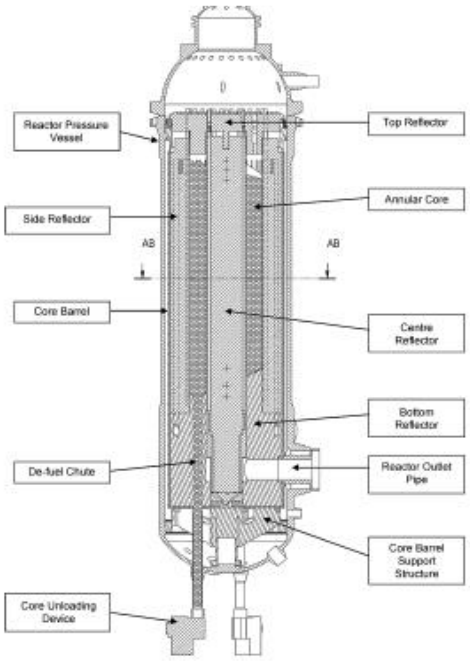

Figure 1. Longitudinal cross-section of the PBMR reactor vessel.

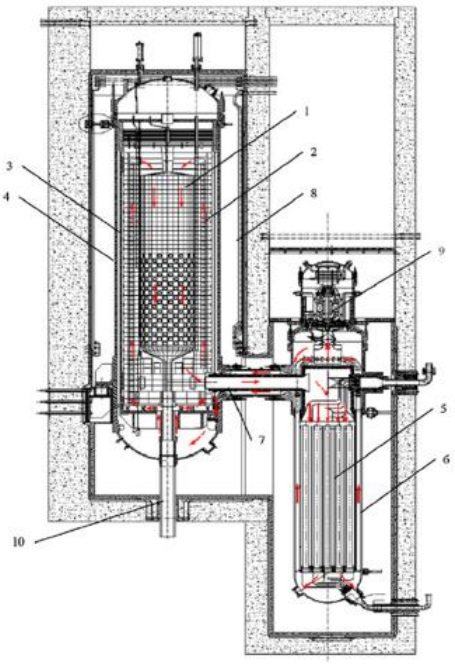

Figure 2. Cross-section of the primary circuit of the HTR-PM.

2. PBMR, HTR-PM and BWR PRESENTATION

Figures 1 and 2 show the two nuclear reactors PBMR by Dudley [1], and HTR PM by Wei [2]. These two nuclear reactors use a spherical fuel and are cooled by helium. The main difference between these two nuclear reactors is at the core level. For PBMRs, the core of the nuclear reactor is annular while the core of the HTR-PM is cylindrical. The designation of the components of each nuclear reactor is given in Figure 1 for the PBMR and in paragraph form after Figure 2 for the HTR-PM.

Cross section of the primary circuit of the HTR-PM. (1) Reactor core; (2) side reflector and carbon thermal shield; (3) core barrel; (4) reactor pressure vessel; (5) steam generator; (6) steam generator vessel; (7) coaxial gas duct; (8) water-cooling panel; (9) blower; (10) fuel discharging tube.

Boiling Water Reactor, BWR, is a nuclear reactor that uses vapor produced directly in the nuclear reactor core without passing through a steam generator. This type of nuclear reactor uses cylindrical fuel and light water (H2O) as moderator and coolant. A description of the components of a BWR is given by Shah, [3].

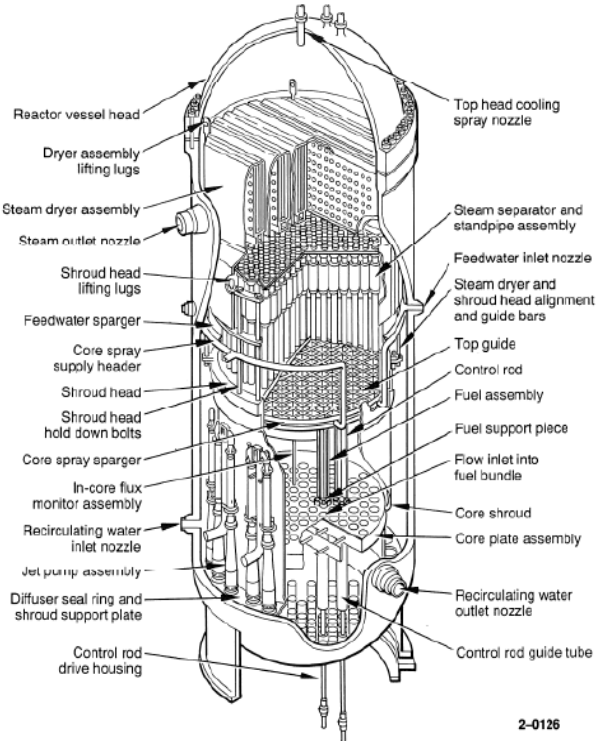

Figure 3. BWR Vessel Internals

Corresponding Author E-mail: kamelsidiali@gmail.com

Acta Materialia Turcica

Volume 4, July 2020, Pages 25-34

3. THEORIES APPLIED TO COMPLEX FLOWS

In this work, a complex flow is defined as a flow where the velocity cannot be calculated in a conventional way.

To do this, two major theories of fluid mechanics are used. The first is the theory of porous media and applies for PBMRs and HTR-PMs knowing that the spherical fuel is deposited in the form of clusters respectively in the annular part for PBMRs and in the central part for HTR-PMs. The flow of the cooling fluide obeys Darcy's law, hence the application of this theory.

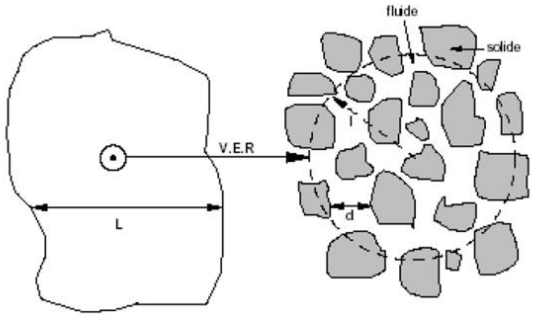

(a) (b)

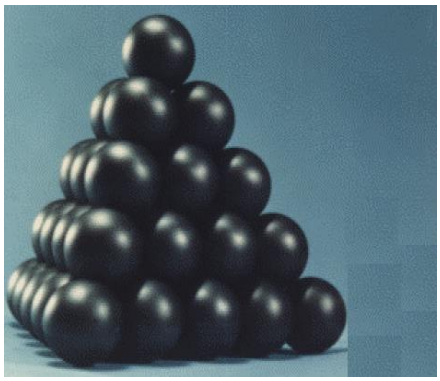

(c)

Figure 4. Porous media. **(a)** Macroscopic, **(b)** Pores scale, **(c)** Disposition of fuel spheres

As for the second theory, it is that of the two-phase flow and is applied to BWRs. The water goes through several flow configurations before ending up in vapor.

The presence of a heat flow through the walls of a vertical pipe changes the flow patterns from those that occur in a pipe with no heat flow for the same flow conditions. According to Collier [4], the different flow configurations in a heated vertical pipe are presented in figure (5) below which gives a schematic representation of a vertical pipe heated by a low and uniform heat flow fed at the base of the liquid.

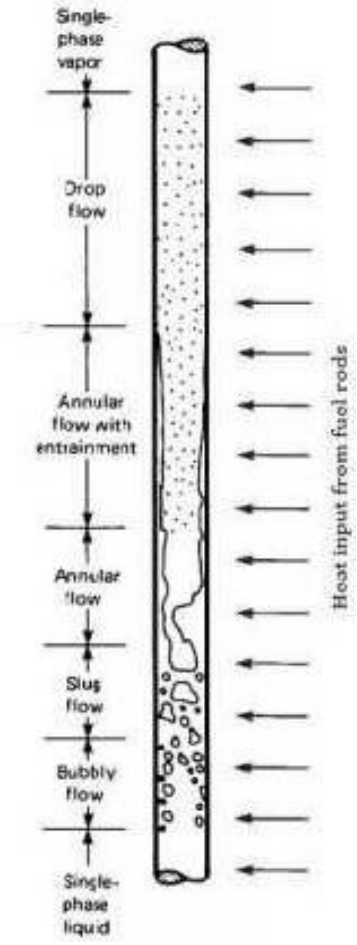

Figure 5. Ascending flow configurations in a heated vertical pipe

In the first region, a single phase of liquid is heated to the saturation temperature for which there is a balance between the liquid phase and the vapor phase for a given pressure. For a wall temperature higher than the saturation temperature of the liquid, the boiling phenomenon takes place, it is defined as a change of state in which the formation of bubbles occurs within the liquid near the wall at a precise temperature, generally at

Corresponding Author E-mail: kamelsidiali@gmail.com

Acta Materialia Turcica

Volume 4, July 2020, Pages 25-34

101 ° C and for a given pressure. Steam bubbles develop and concentrate in the center of the pipe, giving a bubble flow.

The production of more steam leads to a clustering of a large number of vapor bubbles at the center of the pipe to form vapor pockets separated by liquid plugs from the wall. This configuration is called plug flow. The pockets of vapor agglomerate in the center of the pipe to form a vapor core surrounded by the liquid which forms a film in the form of a ring near the wall. It is the annular flow.

The liquid film vaporizes until it disappears completely to form a single-phase vapor flow.

4. PBMR EQUATION SET-UP

In figure 6, is presented a PBMR nuclear reactor core.

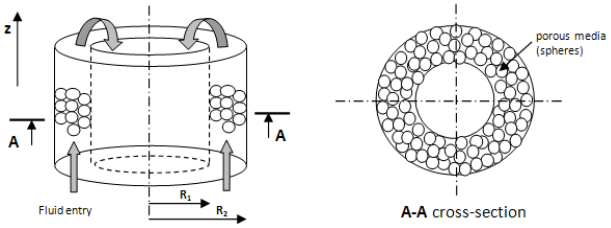

Figure 6. Views of the porous medium in the studied area

Fuel spheres are disposed in the annular portion. The coolant flows from top to bottom by forced convection. The equation set-up, Bounar et al. [5] is based on continuity, momentum and energy conservation equations written in cylindrical coordinates. For continuity, one has:

$$\frac{\partial}{\partial r}(r^* w^*) = 0 \qquad (4.1)$$

where r* is the dimensional radial coordinate and w^* the axial velocity.

For momentum conservation:

$$\frac{\partial p}{\partial r^*} - \frac{\mu}{K} w^* + \left(\frac{1}{r^*}\frac{\partial}{\partial r^*}\left(r^* \frac{dw^*}{dr^*}\right) + \frac{\partial^2 w^*}{\partial z^{*2}}\right)\mu_{eff} = 0 \quad (4.2)$$

As $\frac{\partial^2 w^*}{\partial z^{*2}} = 0$ and putting $G = -\frac{\partial p}{\partial r}$, where μ is the fluid viscosity, K the permeability and μ_{eff} the dynamic viscosity. Introducing the dimensionless variables:

$\eta = \frac{r^*}{D}$, $z = \frac{z^*}{Pe_D D}$, $w = \frac{w^* \mu}{GD^2}$, $Da = \frac{K}{D^2}$, $M = \frac{\mu_{eff}}{\mu}$,

the final equation is written as:

$$\frac{d^2 w}{d\eta^2} + \frac{1}{\eta}\frac{dw}{d\eta} - \frac{1}{MDa} w + \frac{1}{M} = 0 \qquad (4.3)$$

The solution of equation (3) requires a homogeneous solution and a particular solution. For the conservation of energy, and assuming local thermal equilibrium and homogeneity, the energy equation is given by Bejan [6], Kays et al. [7]:

$$\rho c_p w^* \frac{\partial T^*}{\partial z^*} = k\left[\frac{1}{r^*}\frac{\partial}{\partial r^*}\left(r^* \frac{\partial T^*}{\partial r^*}\right)\right] + \emptyset^* \qquad (4.4)$$

where T is the equilibrium temperature of the porous medium, c_p the fluid specific heat, k the effective thermal conductivity of the porous medium and $\emptyset^*$ the viscous dissipation contribution. One introduces the following boundary conditions: $k\left[\frac{\partial T^*}{\partial r^*}\right]_{r=r_1} = q_w$ and $T(r_2) = T_w$ and the dimensionless following parameters:

Br=$\frac{\mu \bar{W}^2}{q_w D}$, θ=$\frac{k(T^* - T_w^*)}{q_w D}$, $\widehat{w} = \frac{w^*}{\bar{W}}$ et $\alpha = \frac{1}{\sqrt{M\,Da}}$,

one gets:

$$\left(\frac{1}{\eta}\frac{\partial}{\partial \eta}\left(\eta \frac{\partial \theta}{\partial \eta}\right)\right) = \widehat{W} f1 + \frac{Br}{Da}\left(\widehat{W}^2 - \frac{1}{\alpha^2}\widehat{W}\left(\frac{1}{\eta}\frac{\partial}{\partial \eta}\left(\eta \frac{\partial \widehat{W}}{\partial \eta}\right)\right)\right) \qquad (4.5)$$

To simplify the calculation of equation (5), an asymptotic series expansion is applied.

5. HTR-PM EQUATION SET-UP

The physical domain, approached by a channel, shown in figure 7, consists of two parallel plates of length l distant from 2H filled with a porous medium saturated with an incompressible viscous fluid entering at a velocity U0 and a uniform temperature T0 with local thermal imbalance. The upper and lower walls are maintained under a constant flow of heat qw. Due to the geometric and physical symmetries, the problem will be

Corresponding Author E-mail: kamelsidiali@gmail.com

Acta Materialia Turcica

Volume 4, July 2020, Pages 25-34

solved for the upper part of the studied domain, Necir et al. [8].

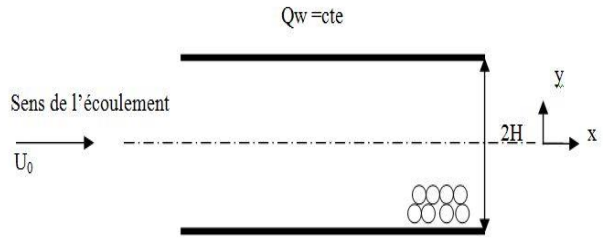

Figure 7. Studied configuration

5.1 Calculation of the Dynamic Field

Continuity equation is written:

$$\frac{\partial u}{\partial x}+\frac{\partial v}{\partial y}=0 \qquad (5.1)$$

The momentum equation is given by :

$$\nabla p+\rho\vec{g}+\mu_{eff}\nabla^2\vec{u}-\frac{\mu}{K}\vec{u}=0 \qquad (5.2)$$

$$\mu_{eff}u\frac{d^2u}{dy^2}-\frac{\mu}{K}u+G=0 \qquad (5.3)$$

where μ_{eff} is the effective viscosity, u the filtration velocity, μ the dynamic viscosity of fluid, K the permeability and G the negative pressure gradient (-dp/dx).

5.2 Calculation of the Thermal Field

The energy equations for the solid phase and the fluid phase are respectively written as follows:

$$k_{s,eff}\frac{\partial^2T_s}{\partial y^2}-h_ia(T_s-T_f)=0 \qquad (5.4)$$

$$k_{f,eff}\frac{\partial^2T_f}{\partial y^2}+h_ia(T_s-T_f)+\frac{\mu u^2}{K}+\mu_{eff}(\frac{du}{dy})^2=\rho c_p u\frac{\partial T_f}{\partial x} \qquad (5.5)$$

6. EQUATION SET-UP FOR BWR FOR THE ANNULAR FLOW CASE

Figure 8 below, shows an annular flow configuration in a vertical pipe with heat transfer to the wall, the liquid forms a ring glued to the wall, and the gas occupies the center of the pipe.

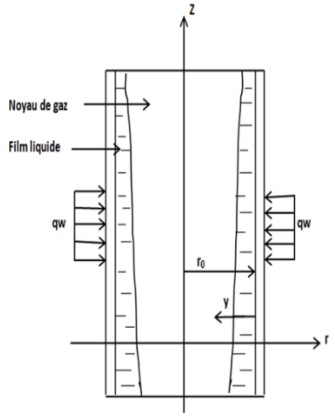

Figure 8. Annular configuration flow

In what follows one presents the different conservation equations, and the empirical relationships used in this model for the prediction of pressure drop, film thickness and heat transfer coefficient, Yasri et al. [9]. The following assumptions are made: the flow is incompressible, the thickness of the liquid film is uniform around the device of the pipe, the pressure is uniform in the radial direction, evaporation occurs at the vapor / liquid interface and last droplets of liquid are distributed uniformly in the core.

At static equilibrium, a balance of the forces exerted on the film is established, Hewitt [10]:

$$dP\frac{\pi}{4}[(D-2\delta)^2-(D-2y)^2]=-\tau_i\pi\,dz\,(D-2\delta)+\tau_L\,\pi\,dz\,(D-2y)-\rho_Lg\,\frac{\pi}{4}\,dz\,[(D-2\delta)^2-(D-2y)^2] \qquad (6.1)$$

With τ_L the shear stress at the wall, τ_i the shear stress at the interface, dP the axial pressure difference between the inlet and the outlet of the pipe, ρ_l the liquid density, g the gravitational acceleration, D the pipe, y The distance from the wall, δ δ the film thickness and dz the pipe length.

According to equation (11) the wall shear stress can be derived from:

$$\tau_L=\frac{1}{2}\left[\frac{dP}{dz}+\rho_Lg\right]\left[\frac{(r_0-\delta)^2-(r_0-y)^2}{(r_0-y)}\right]+\tau_i\left[\frac{r_0-\delta}{r_0-y}\right] \qquad (6.2)$$

With r_0 the radius of the pipe and dP/dz the axial pressure gradient.

Corresponding Author E-mail: kamelsidiali@gmail.com

Acta Materialia Turcica

Volume 4, July 2020, Pages 25-34

The shear stress at the interface can be defined using the equilibrium of forces in the steam core:

$$\frac{dP}{dz}\frac{\pi}{4}[(D-2\delta)^2-(D-2y)^2] = \tau_i\pi\,[(D-2\delta)-(D-2y)] + \rho_v g\,\frac{\pi}{4}\,[(D-2\delta)^2-(D-2y)^2] \quad (6.3)$$

With ρ_v the vapor density.

Equation (13) can be written by replacing the pipe diameter by $(2r_0)$ where r is the pipe radius and dividing by $\pi(D-2\delta)$, one obtains the equation of the interface shear stress in the form of:

$$\tau_i = \frac{1}{2}\left(\frac{dP}{dz}-\rho_v g\right)\left[\frac{(r_0-\delta)^2-(r_0-y)^2}{(r_0-y)}\right] \quad (6.4)$$

The interface shear stress can also be predicted using the correlation given by Wallis [11], which is given by:

$$\tau_i = f_i\ \frac{1}{2}\ \rho_v\, u_v^2 \quad (6.5)$$

With u_v the vapor phase velocity and which is worth$[G\,x/\rho_v]$.

7. APPLICATIONS

7.1 Results and Discussions for PBMR

The obtained results for the dynamic field and the thermal field are presented respectively in figures (9) and (10). In figure (9), for different values of Da = 0.1, 0.3 and 0.5, the distribution of the dimensionless velocity w is obtained as a function of the dimensionless transversal direction η (eta) which varies from 0.27 to 0.5 with a pitch of 0.0575. For a Darcy number equal to 0.1, the variation of the dimensionless velocity increases as a function of η. The dimensionless velocity reaches the maximum value of 0.0075 at η = 0.37 and then decreases as a function of η up to a value that tends to 0. When the Darcy number is equal respectively to 0.3 and 0.5, the value of the dimensionless velocity increases respectively as a function of η up to maximum values of 0.013 and 0.010. This is valid for η = 0.37, then these two curves decrease as a function of η up to a value that tends to 0. Note that the value of the dimensionless velocity w reaches the maximum for different Darcy values at η = 0.37 (center of the channel). In figure (10), the evolution of the dimensionless temperature θ (teta) is presented as a function of the dimensionless transversal direction η (eta) which varies in the same points as for the dynamic field and for a fixed Darcy of 0.001. One notices two things: the first is that when η increases, θ decreases linearly. The second is that the variation of θ is practically the same for the three Brinkman numbers.

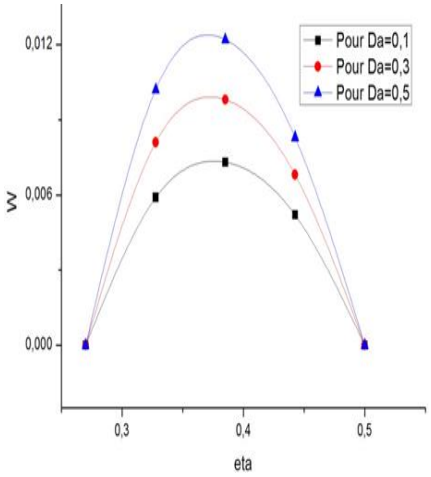

Figure 9. Variation of the dimensionless velocity as a function of η for different Da.

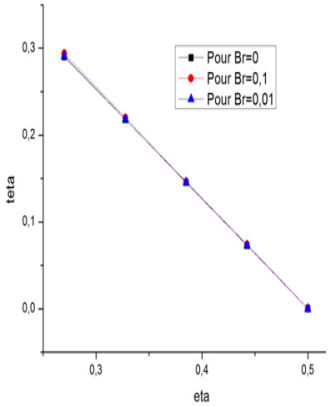

Figure 10. Variation of θ as a function of η for different values of Br and for Da = 0.001.

7.2 Results and Discussions for HTR-PM

The variation of the dimensionless temperature for the two phases θ_f, θ_s as a function of the dimensionless

Corresponding Author E-mail: kamelsidiali@gmail.com

Acta Materialia Turcica

Volume 4, July 2020, Pages 25-34

transverse direction η, Bi, Br, S, k. Each time we vary a dimensionless number and we draw a new curve. We also represent the variation of the number of Nusselt Nu as a function of Br, Bi, S and k, each time we vary a number and we draw a new curve. The obtained results are represented in the following graphs:

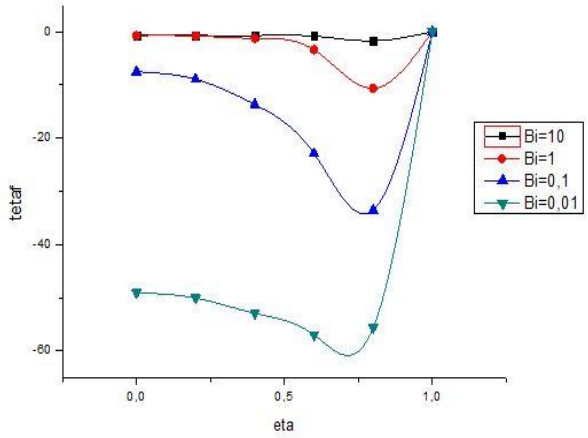

Figure 11. Fluid temperature profile for different Biot number, K=0, 01, S=10, Br=10

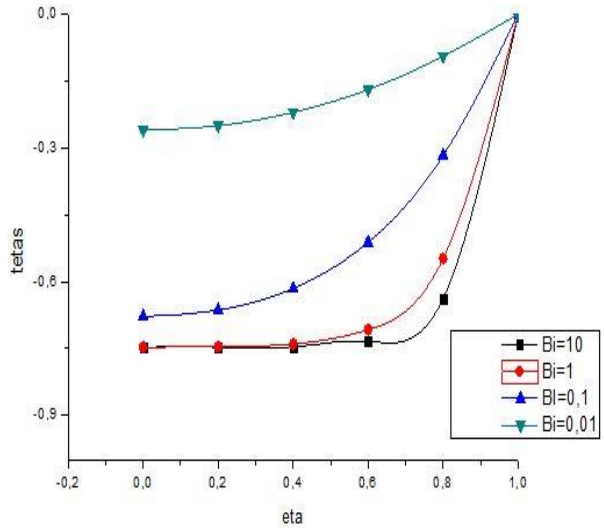

Figure 12. Solid temperature profile for different Biot number, K=0, 01, S=10, Br=10

For both figures (11) and (12), k = 0.01 indicates a high thermal conduction resistance for the fluid relative to that of the solid, S = 10, the flow velocity is nearly uniform except in the thin layer near the walls. The temperature for the solid phase decreases while the temperature of the fluid phase increases for an increase in Biot number. Bi indicates the relative heat resistance of solid conduction to the exchange of internal heat between fluid and solid. For a large Biot value, the external thermal contact is good and the internal heat exchange is efficient. For a small value of Biot the temperature difference between the fluid and the solid becomes smaller. To increase the heat flux transferred from the solid to the walls, there is an increase in the number of Biot or a decrease in the thermal resistance of the internal heat exchange. This lowers the temperature of the solid while the fluid temperature increases and approaches the temperature of the solid for an increase in the number of Biot. Hence, the transfer of total heat is dominated by solid conduction when $k \ll 1$ and an increase in Biot number.

7.3 Results and Discussions for BWR (annular flow case)

In figure (13) and (14) one sees the evolution of the pressure gradient as a function of the mass velocity at different quality values ranging from 0.05 to 0.15 with a pitch of 0.02 and vice versa. This variation is given at a mass velocity varying from 1 Kg/m2s up to 400 Kg/m2s. As the mass velocity increases, the pressure gradient increases and it also increases as the vapor quality increases.

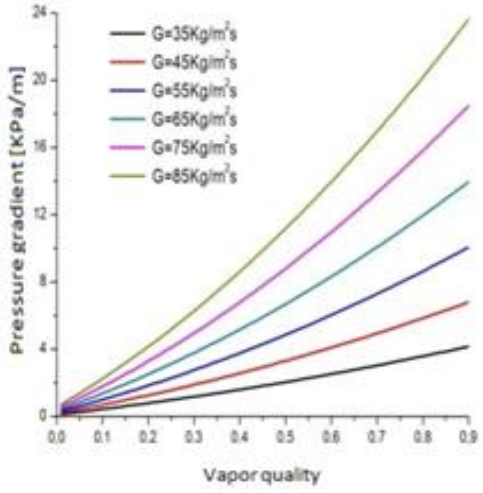

Figure 13. Pressure gradient evolution function of quality for different massic velocities

Corresponding Author E-mail: kamelsidiali@gmail.com

Acta Materialia Turcica

Volume 4, July 2020, Pages 25-34

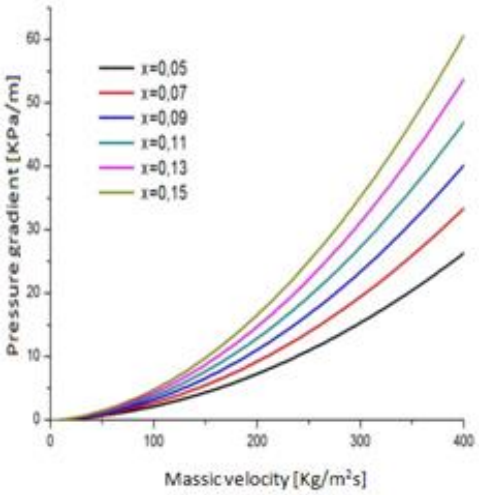

Figure 14. Pressure gradient evolution function of massic velocity for different qualities.

Figure (15) below, shows the evolution of the liquid film thickness as a function of the vapor quality at different values of the mass velocity.

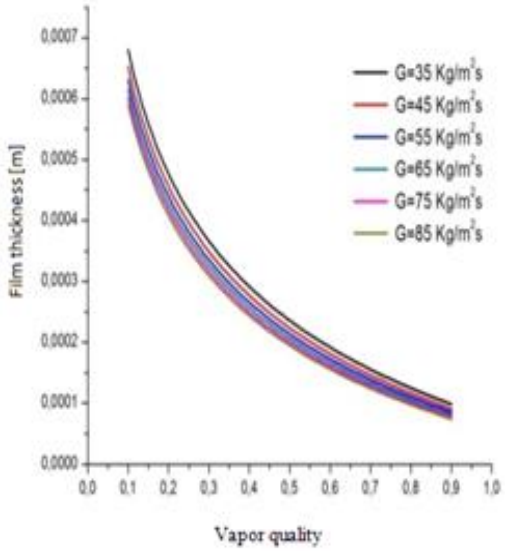

Figure 15. Film thickness evolution function of quality for different mass velocities

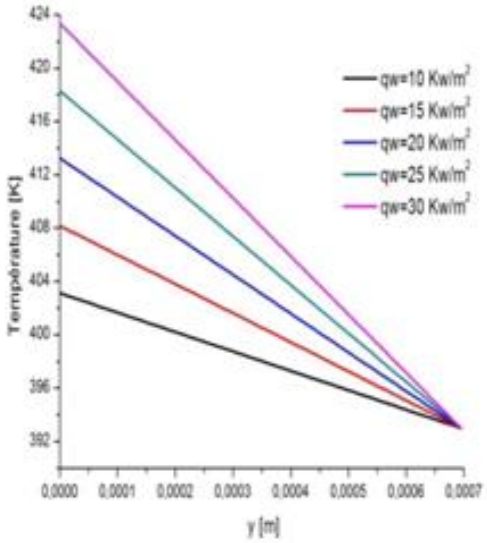

Figure 16. Temperature distribution function of the distance from the wall to the liquid-vapor interface

It can be seen that the thickness of the film decreases when the quality of vapor increases and it also decreases when the mass velocity is increased, this is due to the increase in the flow rate of the vapor and the decrease in that of the liquid by evaporation which causes the decrease of the thickness of the film. At a saturation temperature of 393 K, a vapor quality of 0.1 and a mass velocity of 35 Kg/m^{2}s, we have the distribution of the temperature in the film which is presented in figure (16) as a function of the distance y which varies from the wall to the thickness of the film and which is 0.000695 m and by varying the heat flux at the wall from 10 KW/m^2 up to 30 KW/m^2. The evolution of the temperature varies linearly until it reaches the saturation temperature which is 393 K. The decrease of the temperature is proportional to the quantity of heat flux, the more the heat flow is increased the more the temperature of the wall increases.

Figure (17) shows the evolution of heat transfer coefficient as a function of the vapor quality for several values of the mass velocity. By making the mass velocity vary from 35 Kg/m^{2}s up to 85 Kg/m^{2}s and the quality from 0.1 up to 0.9 the heat transfer coefficient increases with the increase of these, it is due to the decrease of the film thickness.

Corresponding Author E-mail: kamelsidiali@gmail.com

Acta Materialia Turcica

Volume 4, July 2020, Pages 25-34

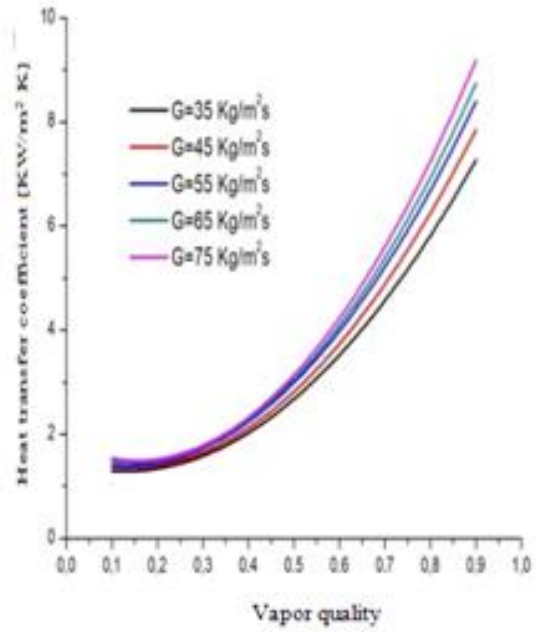

Figure 17. Heat transfer coefficient variation function of quality for different mass velocities

8. CONCLUSIONS

8.1 For PBMR

Using asymptotic methods, the dynamic and thermal fields were determined in a porous medium contained in an annular configuration corresponding to the PBMR nuclear reactor core. The results obtained showed that the dynamic field evolves according to the evolution of the Darcy number whereas the thermal field, for a constant Darcy, decreases linearly for increasing values of η. It has also been found that the Brinkman number for a constant Darcy does not affect the variation of the dimensionless temperature θ. The model developed and solved gives physically valid results.

8.2 For HTR-PM

Convective heat transfer in a channel filled with a porous medium depends on several parameters such as the Biot number Bi, the ratio of the effective thermal conductivities k, the Brinkman number Br and the porous medium form factor S. Nu variation depends on the thermal resistance of the fluid and solid conduction and also on the interstitial heat exchange. The strong dependence of Nu on Br, S, Bi, and k verifies the significance of considering the viscous dissipation effects in the thermal energy equation for a model of two equations. It is stated that the frictional heat generation is confined in the vicinity of the walls while the heat generation due to the internal heating occupies a large portion of the porous medium from the center of the channel.

8.3 For BWR

In order to predict the pressure drop, film thickness and heat transfer coefficient in an upward annular two-phase flow in a vertical pipe with wall heating, the phase-separated model was used, the equations of Continuity, momentum and energy are used to calculate the pressure gradient and the heat transfer coefficient, they have been solved analytically.

The presence of a heat flux at the wall modifies the main parameter of the flow which is the film thickness, the results obtained show the influence of the vapor quality and the mass velocity on the heat transfer coefficient and the film thickness as well as on the pressure drop. The pressure gradient and the heat transfer coefficient increase with the increase of the vapor quality and the mass velocity while the thickness of the film decreases with the increase of the latter, the temperature profile decreases linearly from the wall temperature up to the saturation temperature. This physically correct behavior makes it possible to predict the amount of steam produced as a function of all the physical quantities studied in this work.

9. GENERAL CONCLUSION

The results show that the Darcy number and the Brinkman number have a direct influence on the fluid temperature and velocity in a PBMR. This can be extrapolated to any type of nuclear reactors using pebble bed configuration. For HTR-PM, it can be said that in the case of a thermal non-equilibrium, the dimensions ratio plays an important role in monitoring the temperature of the coolant and the temperature of the fuel. As for BWR, the results during the annular flow show that the liquid thickness is the main parameter which governs the evolution of all the thermal hydraulic parameters. The obtained results, presented in figures and physically analyzed, are very satisfactory. It can thus be concluded

Corresponding Author E-mail: kamelsidiali@gmail.com

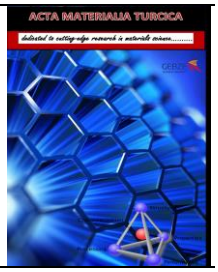

that applying the model of porous media and the two-phase flow one for complex fluid flows respectively for PBMR, HTR-PM or BWR power nuclear reactors cores can ensure a good thermal hydraulics behavior.

10. REFERENCES

[1] Xu Wei, Sun Jun, Zheng Yanhua, Shi Lei, The influence of nuclear graphite oxidation on air accident of HTR-PM, Annals of Nuclear Energy, 110 (2017) 1242-1248.
DOI: https://doi.org/10.1016/j.anucene.2017.08.028

[2] T.Dudley, W. Bouwer, P. de Villiers, Z. Wang, The Thermal–Hydraulic model for the pebble bed modular reactor (PBMR) plant operator training simulator system, Nuclear Engineering and Design, 238 (2008) 3102–3113.
DOI: https://doi.org/10.1016/j.nucengdes.2007.12.022

[3] V. N. Shah, and P. E. MacDonald, Aging and Life Extension of Major Light Water Reactor Components, Elsevier Science, Atlanta,1993.

[4] J.G. Collier and J. R. Thome, Convective boiling and condensation, third ed., Oxford Science Publications, Oxford, 1994.

[5] M. Bounar, A. Necir, K. Sidi-Ali, Kh. Bouhadef, Heat transfer evolution in a porous medium; dynamic and thermal fields calculations for high temperature nuclear reactors, Algerian Congress of Mechanics, Ghardaia, 2019.

[6] A. Bejan, Convection Heat Transfer, Wiley, New York, 2004.

[7] W. Kays, M. Crawford, B. Weigand, Convective Heat and Mass Transfer, McGraw Hill, New York, 2005.

[8] A. Necir, M. Bounar, K. Sidi Ali, Kh. Bouhadef, Kh. Oukil, Etude de la convection forcée dans un canal poreux avec effets de la dissipation visqueuse, 9èmes Journées de Mécanique, Bordj El-Bahri, 2014.

[9] I. Yasri, M. A. Alreme, K. Sidi-Ali, A. Boumedien, Prédiction de la Chute de Pression et du Transfert de Chaleur Dans un Ecoulement à Deux Phases Annulaire Ascendant, 9èmes Journées de Mécanique, Bordj El-Bahri, 2014.

[10] G.B. Wallis, One-dimensional Two-phase Flow, McGraw-Hill, New York, 1969.

[11] G. F. Hewitt, N.S Hall-Taylor, Annular Two-Phase Flow, Pergamon, New York, 1970.

Corresponding Author E-mail: kamelsidiali@gmail.com